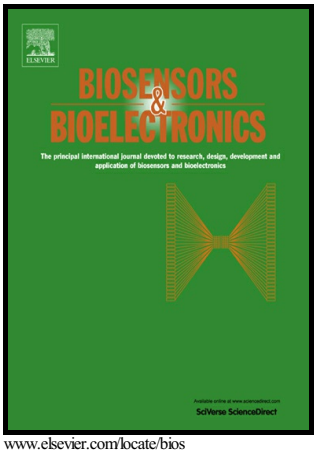

www.elsevier.com/locate/bios

Impedimetric array in polymer microfluidic cartridge for low cost point-of-care diagnostics

Andrew Lakey, Zulfiqur Ali, Simon M. Scott, Syrine Chebil, Hafsa Korri- Youssoufi, Santha Hunor, Anna Ohlander, Mathias Kuphal, Josep Samitier Marti

PII: S0956-5663(19)30022-3
DOI: https://doi.org/10.1016/j.bios.2018.12.054
Reference: BIOS11026

To appear in: *Biosensors and Bioelectronic*

Received date: 15 October 2018
Revised date: 12 December 2018
Accepted date: 20 December 2018

Cite this article as: Andrew Lakey, Zulfiqur Ali, Simon M. Scott, Syrine Chebil, Hafsa Korri- Youssoufi, Santha Hunor, Anna Ohlander, Mathias Kuphal and Josep Samitier Marti, Impedimetric array in polymer microfluidic cartridge for low cost point-of-care diagnostics, *Biosensors and Bioelectronic,* https://doi.org/10.1016/j.bios.2018.12.054

Impedimetric array in polymer microfluidic cartridge for low cost point-of-care diagnostics

Andrew Lakey[a], Zulfiqur Ali[a*], Simon M. Scott[a], Syrine Chebil[b], Hafsa Korri- Youssoufi[b], Santha Hunor[c], Anna Ohlander[d], Mathias Kuphal[e], Josep Samitier Marti[e],

[a]Healthcare Innovation Centre, Teesside University, Middlesbrough, Tees Valley, TS1 3BX, UK

[b]Equipe de Chimie Bioorganique et BioInorganique (ECBB), Institut de Chimie Moléculaires et des Matériaux d'Orsay (ICMMO), UMR-CNRS 8182, Univ Paris Sud, Université Paris-Saclay, 91405 Orsay, France

[c]Department of Electronics Technology, Budapest University of Technology and Economics, Budapest, Hungary

[d]Fraunhofer EMFT, Institution for Microsystems and Solid State Technologies, Munich, Germany

[e]IBEC-Institute for Bioengineering of Catalonia, Barcelona Institute of Science and Technology (BIST), Barcelona, Spain

ABSTRACT

Deep Vein Thrombosis and pulmonary embolism (DVT/PE) is one of the most common causes of unexpected death for hospital in-patients. D-dimer is used as a biomarker within blood for the diagnosis of DVT/PE. We report a low-cost microfluidic device with a conveniently biofunctionalised interdigitated electrode (IDE) array and a portable impedimetric reader as a point-of-care (POC) device for the detection of D-dimer to aid diagnosis of DVT/PE. The IDE array elements, fabricated on a polyethylenenaphtalate (PEN) substrate, are biofunctionalised in situ after assembly of the microfluidic device by electropolymerisation of a copolymer of polypyrrole to which is immobilised a histidine tag anti-D-Dimer antibody. The most consistent copolymer films were produced using chronopotentiometry with an applied current of 5μA for a period of 50 seconds using a two-electrode system. The quality of the biofunctionalisation was monitored using optical microscopy, chronopotentiometry curves and impedimetric analysis. Measurement of clinical plasma sample with a D-dimer at concentration of 437 ng/mL with 15 biofunctionalised IDE array electrodes gave a ratiometric percentage of sample reading against the blank with an average value of 124±15 at 95% confidence. We have demonstrated the concept of a low cost disposable microfluidic device with a receptor functionalised on the IDE array for impedimetric detection towards POC diagnostics. Changing the receptor on the IDE array would allow this approach to be used for the direct detection of a wide range of analytes in a low cost manner.

Key words: Impedimetric sensing; electropolymerisation; interdigitated electrodes; point-of-care diagnostics; microfluidics

1.0 Introduction

Venous thromboembolism (VTE) is a condition in which the blood clots inappropriately and causes considerable morbidity and mortality in all ethnicity, genders and ages (Beckman et al., 2010). VTE is a disease which can manifest as either pulmonary

embolism (PE) or deep vein thrombosis (DVT)(Lopez, 2004). PE is often accompanied by, or preceded by the development of DVT (Chan and Ginsberg, 2002). VTE is the third most common life-threatening cardio vascular disease in the USA (Cushman et al., 2004) and with many of the known risk factors (advanced age, immobility, surgery, obesity) increasing within society it is a growing public health concern. Venography is considered to be the gold standard method of diagnosing DVT but this is an invasive procedure (Bucek et al., 2001). Alternative non-invasive techniques including doppler ultrasound and computed tomography (CT) (Srivastava et al., 2004) are relatively time consuming and expensive to perform.

The fragments of a clot are called fibrin degradation products (FDP) and one of these is D-dimer which consists of two cross-linked D fragments of the fibrinogen protein (Bourigua et al., 2010). Elevated levels of D-dimer is indicative of numerous conditions (including VTE) that lead to the activation of coagulation and fibrin formation (Ghanima and Sandset, 2007). There has been a growing interest in the development of D-dimer based enzyme-linked immunosorbent assays (ELISAs). Although D-dimer based ELISAs have demonstrated a high sensitivity and negative predictive value (NPV) they are also extremely labour intensive, time consuming and are designed for batch analysis (Božič et al., 2002). D-dimer electrochemical ELISA's have been demonstrated on microfluidic devices (Rossier and Girault, 2001) with the antibodies immobilised to the surface of a photo-ablated microchannel prior to D-dimer interaction. The detection in this instance uses a secondary HRP labelled antibody for the enzymatic conversion of hydroquinone in the presence of hydrogen peroxide. This sensor yields a detection limit of ~100pM and a dynamic range (0.1-100nM) three orders of magnitude larger. This is of particular clinical interest as the cut off range for early stage thrombosis/embolism is around 400ng/mL (2nM). Despite the promise of this microfluidic electrochemical ELISA, it still suffers from problems such as the need of a secondary labelled antibody, which can influence the cost and ease of the measurement.

Direct electrochemical detection of D-dimer could be achieved through various transducers. Potentiometric detection of D-dimer has been demonstrated with silver nanoparticles decorated ZnO nanotubes (Ibupoto et al., 2013), ZnO nanorod (Ibupoto et al., 2014) and graphene (Nikoleli et al., 2014). Impedimetric detection has been demonstrated to offer several advantages such as, ease of use, rapid and sensitive response (Prodromidis, 2010; Santos, 2014). A key advantage of using impedance over many other methods is the potential ability to perform direct label-free detection. Most other methods attach a label (e.g. fluorophore or chromophore) to the target and the label is then detected and related to the amount of bound targets. Use of a label on a biomolecule has the drawback of altering its binding properties and the target-label coupling reaction can be variable, which can be a particular issue for protein targets. A label can allow higher selectivity and or sensitivity but this is often at the expense of additional cost, time and sample handling. Several impedimetric immunosensors have been reported for D-dimer detection that involved SWCNTs (Bourigua et al., 2010), MWCNTs (Chebil et al., 2013), and Chitosan/Gold nanoparticle (Rodrigues et al., 2018). We have previously described impedimetric immunosensor detection using conducting copolypyrrole film to which a histidine tag antibody has

been bound using a complex NTA chelator coordinated with copper as metal. A model antigen was determined in the range of 0.1-10ng/mL by measuring the charge transfer resistance (Rct) of the biolayer at the reduction potential of copper (Hafaid et al., 2010). We subsequently demonstrated the detection of D-dimer in the range of 0.1-500 ng/mL, with a limit of detection of 100pg/mL (Chebil et al., 2010).

The integration of biosensors into microfluidic devices with array of electrodes and reader able to convert the biological information of detection remains a significant challenge for development of POC systems (Rackus et al., 2015). There are few examples of POC system integrating such components. These include a system with DNA amplification and detection chambers with two electrode array (Ferguson et al., 2009) and a microfluidic system with microelecrode array based on amperometric competitive immunoassay for prostate specific antigen (Triroj et al., 2011). A further example includes DNA detection based on integrated biosensors modified with MWCNTs and where the integration in microfluidic system improves the sensitivity of detection and leads to a lower detection limit (Zribi et al., 2016).

Here we describe use of an array of IDEs within a microfluidic cartridge manufactured using high volume and low-cost approach and a portable impedimetric reader for immunosensor D-dimer detection. The biofunctionalisation approach of the IDEs is based on electropolymerized polypyrrole and antibody immobilization through NTA/Copper complex. This allows the individual functionalisation of the array elements through electrochemical patterning of polypyrrole. The overall approach adopted has potential for the development of a low cost POC system for the detection of D-dimer for DVT/PE. Changing the immobilised receptor and the electric field, through modifying the IDE transducer configuration, would allow this to be developed as a generic low cost diagnostic approach for direct monitoring of a wide variety of ligand/receptor binding events. This could include use of aptamers for small molecules to DNA/RNA hybridisation to the detection of viruses and bacteria (2-5μm particles).

2.0 Materials and Methods

2.1 Instrumentation

Electropolymerisation of the electrodes and electrochemical measurements were performed using the Auto LAB potentiostat/galvanostat (Eco Chemie B.V.) in conjunction with General Purpose Electrochemical System (GPES) software and Frequency Response Analyzer (FRA) software (Eco Chemie B.V.) for electropolymerisation/cyclic voltammetry (CV) and electrochemical impedimetric measurements respectively.

A portable impedimetric reader system was developed for the microfluidic cartridge with IDE array but a separate connector frame was designed and fabricated for the preliminary measurements and for the biofunctionalisation processes. The connector frame included two red LEDs (powered by a 9V battery) to allow quick connection and accurate alignment of the microfluidic cartridge with the spring-loaded connector pins (Figure 1A) with the AUTOLAB system for the polymerisation process and analysis of the functionalised bio-layer. The meander shaped working electrodes were individually

addressed for connection, whilst the interdigitated fingers (counter electrodes) were grouped as a single connection.

2.2 Microfluidic cartridge with IDE array

The microfluidic cartridge comprises a three-layer structure with a microfluidic channel layer and electrode layer that are joined by an adhesive layer (Figure 1). The microfluidic channel layer was fabricated from a polycarbonate sheet (3.0mm) by hot embossing (Jenoptik Mikrotechnik Hex 02).

The electrode layer comprised a five element IDE array (30µm finger width and spacing), four resistive elements for fluid localisation and two platinum temperature sensor elements on a 125µM PEN sheet. Gold electrodes were fabricated by physical vapour deposition (PVD) by sputtering a 250 nm gold layer (Au) with subsequent patterning using photolithography as described previously (Kuphal et al., 2012). An extra metal layer (e.g. chrome or titanium), to promote metal adhesion, was not necessary in this case as the gold was found to adhere sufficient well directly to the polymer. Each set of IDEs consisted of two interdigitated electrodes as the counter electrode and a third 'meander' electrode which is employed as the working electrode in the system. The temperature is determined by measuring the resistance of platinum electrode incorporated on the PEN substrate. A constant current is driven through the resistor and the voltage drop across the resistor is measured using a 4-wire set-up so that the error caused by the resistance of the measuring wire is eliminated.

The electrode and microfluidic channel layers were joined in a two-step lamination process using an optical alignment system with a 50µM thick double-sided adhesive tape (AR care 8890, Adhesive Research Ireland Ltd), primarily chosen for its high shear strength. The adhesive tape was laser cut with the outer contour of the microfluidic cartridge and the inner contour of the microfluidic channel.

2.3 Electropolymerisation

Prior to electropolymerisation, the IDE array in the microfluidic cartridge was rinsed three times with pure ethanol to remove any material from the electrode surface. Electropolymerisation was performed using both chronoamperometry and chronopotentiometry (galvanostatic) approaches. Monomer solution (8mM pyrrole (Py)/ 2mM Nhydroxyphtalimide pyrrole (PyNHP)/0.5M $LiClO_4$ in ethanol) was placed in the microfluidic chamber with the IDE array. Chronoamperometry was performed at 0.9V vs. Ag/AgCl reference electrode (external to the microfluidic cartridge) for 200 seconds or until a maximum charge of 11mC/cm^2 was obtained to give the copolymer films (Py-PyNHP). Chronopotentiometry was performed at 5µA for 50 and 100 seconds. In all cases, after electropolymerisation of the IDE array, the microfluidic cartridge was rinsed with ethanol three times to remove excess monomer solution, followed by rinsing with deionised water three times.

An increase in the sensor sensitivity was attempted by increasing the surface area using gold nano-particles (Au-NP). A solution of 0.5M gold nanoparticles ($K_2Au(CN)_6$) in PBS was injected into the microfluidic chamber, Au-NPs were deposited onto the IDEs using chronoamperometry. In order to deposit AuNPs onto the IDEs by

electrodeposition, a -1V potential was applied for 10 seconds followed by a 0V potential for a duration of 100 seconds and the procedure repeated twice. The IDEs were analysed using differential pulse voltammetry in a solution of 1mM $K_3Fe(CN)_6$/ 1mM $K_4Fe(CN)_6$ in PBS.

2.4 Bio-functionalisation Process

The formation of the bio-layer (SI figure 1) on the IDE array within the microfluidic device was achieved by firstly injecting 7mM (pH 9) NαNα-Bis(carboxylmethyl)-L-lysine hydrate (NTA) in PBS into the microfluidic cartridge for one hour in order to attach the ligand NTA group to the PyNHP group in the polymerised film. The microfluidic cartridge was again rinsed three times with deionised water prior to the formation of the NTA/Cu^{2+} complex, which was achieved by injecting 3.5mM copper acetate in the microfluidic cartridge for 20 minutes. Residual copper was removed by rinsing three times with deionised water before immobilization of a histidine tagged anti-D-dimer antibody (8µg/ml) for 30 minutes. Casein (50µg/ml) was used to block the remaining surface to prevent non-specific absorption. Analysis of the formed bio-layer was performed using electrochemical impedimetric measurements in PBS buffer (applied potential 0V).

2.5 Clinical measurements

A plasma sample containing D-dimer was taken from a clinical sample pool at a concentration of 437 ng/ml and validated with Pathfast Immunoanalyser (Mitsubishi Chemical Europe). Measurements were made with the in-house developed portable impedimetric reader into which is inserted the microfluidic cartridge with biofunctionalised IDE array. First, baseline measurements were made on the IDE array in the microfluidic cartridge. The electrolyte was then washed and replaced by the clinical sample for 15 minutes incubation.

3.0 Results and Discussion

3.1 Portable impedimetric reader system

The in-house developed portable impedimetric reader was based on the AD5933 chip from Analog Devices. The excitation signal over the 20 Hz - 10,000 Hz range was covered with 4 adjustable amplitudes (20, 40, 100 and 200 mV). The usable (presettable) mesurement ranges were the charge resistance (R_{ct}) = 4,7 or 10 or 100 or 470 kOhm and double layer capacitance (C_{dl}) = 220, 470, 100 and 68 nF. The portable device was capable of measuring biofunctional layers with similar ranges of values. Between the 100 kOhm - 1 MOhm R_{ct} range of a PCB dummy of biosensor layer charge transfer resistance our device had ca. 2% error in each of the 5 measurement channels (IDEs) and with the relative standard deviations of ca. 0.5 % for 1MOhm and 0-0.01 % for the 100 kOhm. The input ports of the circuitry are connected to the five working electrodes (WEs) of the microfluidic cartridge via an inverting amplifier and an analog matrix switch. The input ports of the circuitry can be connected to any of the working electrodes individually or to all of them simultaneously. The DC voltage of the working electrodes is adjusted by a D/A convertor connected to the non-inverting input port of the amplifier. The impedance measurement unit was also used to measure the

impedance of four pairs of fill sensors that are integrated within the microfluidic cartridge. The measurement is based on Nyquist plot followed by fitting of data with equivalent circuits where the Rct is in parallel with Cdl and all in series with Rs as the resistance of solution. The Warburg impedance is not observed since at high frequencies, the Warburg impedance is small given that the diffusing reactants are not required to move very far. In addition, the small dimension of the electrode as well as the small volume chamber improve diffusion that could be similar to spherical one.

The impedimetric reader includes a liftable tray to provide the fluidic and electric connections with the microfluidic cartridge. Contact between the electrodes integrated in the microfluidic cartridge and the impedimetric reader is achieved by means of 2 rows of spring-tip electrodes. The liftable tray functions to align the microfluidic cartridge in working position, prevent its' movement and ejection after the assay is completed. The impedimetric reader makes fluidic contact of buffer solution with the microfluidic cartridge by means of a needle, which penetrates a resilient septum on the microfluidic body. The fluidic contact was sufficiently tight for single use of the microfluidic cartridge as is the intended use.

3.2 Fabrication of the DVT/PE POC microfluidic cartridge

A key objective for the fabrication approach for the polymer microfluidic cartridge with the impedimetric IDE array was for development of a device that would have potential for high volume and low-cost manufacture. Moreover, the use of an impedimetric IDE array has the advantage of either replicate measurements of a single biomarker in the microfluidic cartridge and or detection of multiple biomarkers. The IDE array fabricated on a PEN polymer substrate offers the potential for high volume and low-cost manufacture using a roll-to-roll or other high volume single sheet processes. The microfluidic channel layer was fabricated using hot embossing that can be used for volume production of devices. For higher volume production of devices then the hot embossing approach could be substituted with a micro-injection moulding approach.

A major challenge for assembly of the polymer microfluidic cartridge was for accurate alignment which for the channel and electrode geometry was required over a distance of more than 55mm and is beyond what is normally required for Si chip bonding. For a polymer based device this is made more difficult because of the poorer dimensional stability of polymers with the chemical and thermal changes that will arise due to the lithographic processing of the electrode layer and the hot embossing for the microfluidic channel layer. The dimensional variance of the polymer microstructure makes the alignment a more critical element if a mismatch of the layers is to be avoided with the associated distortion of the channel geometries and disturbance of the fluid flow properties. The accuracy of the alignment was determined by the position of the resistive electrodes, incorporated for liquid fill sensing, with respect to the microfluidic channel. The more significant mismatch arose from the thermal shrinkage of the polycarbonate microfluidic channel layer during the hot embossing process. The assembly approach was able to achieve an alignment accuracy of 34±19µm in the lateral and 34±18µm in the horizontal directions. The microfluidic cartridge was able to hold fluid without any leakage. More generally, however, it is clear that an intermediate laminate bonding film can be an appropriate approach for

creation of a hybrid material system where the two materials are incompatible for thermal or solvent bonding but independently have desirable manufacturing and performance characteristics.

The contact pads for the IDE array, flow control electrodes for fill sensing and temperature sensor are situated at the long edges of the microfluidic cartridge. At these edges, the electrode layer is wider than the microfluidic body which allows access of the impedimetric reader to the contact pads and functional integration and control of the electrodes by the reader. A septum is attached to the microfluidic body by means of an adhesive. Care needs to be taken that the surface of the microfluidic body is smooth over the whole surface area of the septum to avoid leakage of liquid.

3.3 Electropolymerisation and biofunctionalisation of the IDE array in the microfluidic cartridge

Functionalisation of the IDE array could be carried out either before or after bonding of the PEN IDE array layer with the microfluidic channel layer. We adopted to functionalise within the microfluidic cartridge since this has the advantage of passivation of the electrodes which makes it easier to select the individual IDE elements for functionalisation. A drawback is, however, that the IDE array elements within a microfluidic cartridge have significantly higher resistivity values. The previously described chronoamperometry approach (Chebil et al., 2010; Hafaid et al., 2010) used for polymerisation on IDEs within the microfluidic cartridge showed large differences for the different IDEs. Subsequent biofunctionalisation of the IDEs also resulted in very different Nyquist plots for the different IDEs which will have arisen in significant part from the variability of the initial electropolymerisation process. Thus, an alternative chronopotentiometry (galvanostatic) polymerisation approach was investigated using an applied current of 5μA for periods of 50 and 100 seconds with an external reference electrode. From the polymerisation curves, a constant current at 100 seconds seemed to show better reproducibility as shown in the curves of variation of potential within time for the IDEs in the microfluidic cartridge (Figure 2). After biofunctionalisation, DPV was used to measure the redox signal of copper complex where an more apparent oxidation peak for Cu^{2+} ion was obtained in the case of 100s time polymerisation (SI figure 2).

In respect of the detection properties, impedimetric analysis, however, showed a decrease in the charge transfer resistance, observed by decrease of diameter of the Nyquist semi-circle, with addition of D-dimer protein (1ng/ml and 0.1μg/ml) for IDEs formed with constant current at 100 seconds against an increase in charge transfer region for a biolayers formed with application of a constant current at 50 seconds (Figure 3). An increase in charge transfer resistance can be expected with addition of antigen since there will be additional resistance to electron transfer arising from the complex antigen-antibody formation. The thick film of polypyrrole formed with 100s time appears less sensitive to the complex formation. This result is in concordance of the previous published work with polypyrrole as transducer where it was demonstrated that thin films are more sensitive to biocomplex formation (Korri-Youssoufi and Yassar, 2001). As a consequence, further studies for the formation of the biolayer on IDEs using chronopotentiometry employed a constant current of 5μA for

50 seconds. It should also be noted that there is a negligible difference in the charge transfer between addition of antigen from 1ng/ml to 0.1μg/ml. This is ascribed to a saturation of the biosensor element so that there are insufficient available antibodies to bind with the higher concentration of antigens.

Electro-deposition of Au-NPs was performed in order to study the effect of increasing the surface to volume ratio on the biolayer sensitivity. This approach attempts to improve sensor surface and also facilitate electron transfer as demonstrated previously (Tertiş et al., 2017). The Au-NP coated IDE showed an approximate four times increase in the surface compared to the untreated electrode surface as demonstrated with the intensity variation of redox current of SWV obtained with $K_3Fe(CN)_6$ redox couple (SI figure 3A). The electro-deposition also resulted in a shift in the peak potentials of Fe^{2+}/Fe^{3+} redox couple at lower potential of 300 mV compared to untreated IDE. This is attributed to a higher electron transfer ability obtained after deposition of Au-NPs that increases both the surface to volume ratio and also the conductivity of the surface electrode compared to the untreated IDE. Subsequent biofunctionalisation and addition of D-dimer antigen, however, showed no increase in the charge transfer after complex formation (SI figure 3B). This is attributed to an increase of the surface density of the polypyrrole layer on the IDE electrode and consequently a higher density of the antibody attached leading to steric effects. As a result of this, Au-NPs were not further employed for biofunctionalisation within the microfluidic cartridge for the clinical sample measurements.

The biofunctionalised IDE arrays were tested with varying concentrations of D-dimer using DPV (SI figure 4). A decrease of the current density corresponding to the redox probe signal for the Cu^{2+}/Cu^{+} indicates good fixation of the D-dimer antigen on the anti D-dimer antibody. We also studied the effect of potentially interfering molecules present in blood with the biofunctionalised IDE array. Non-specific responses from relatively high concentration of haemoglobin, billubirin, heparin and triglyceride were found to be modest indicating specificity of the antibody and effectiveness of the treatment of the biolayer by casein to prevent non-specific interaction.

3.4 Reproducibility of biofunctionalisation on microfluidic IDEs array

Reproducibility of the functionalised IDEs within the microfluidic cartridge was higher by electropolymerisation using a two-electrode system than with a three-electrode system, which includes an external Ag/AgCl reference electrode (Figure 4). It is thought that the relatively small spacing between the IDE fingers negates the requirement for a reference electrode. Electropolymerisation using the two electrode system was therefore chosen for all further development. A number of publications have previously demonstrated conductimetric detection on IDEs without the use of a reference electrode (Anh et al., 2004; Jaffrezic-Renault and Dzyadevych, 2008; Khadro et al., 2008; Marrakchi et al., 2005).

The quality of biofunctionalisation is dependent on the quality of the surface of the bare IDEs and this could be ascertained through optical microscope images of the IDEs. Figure 5 (I) shows bare IDEs with either contamination or residual connection between the counter and working electrodes arising from incomplete etching, the latter giving

rise to flat polymerisation curves. This can lead to biofunctionalisation of the meander which is patchy or inhomogeneous as opposed to a uniform green coating that is obtained from IDEs with a good surface quality. The errors that arise in the operation of the microfluidic cartridge will be a combination of errors from the three main steps in the manufacture of the microfluidic cartridge, namely: manufacture of IDEs, assembly of the microfluidic cartridge and biofunctionalisation. The potential over the electropolymerisation cycle (50 seconds) was used as a metric for measuring the quality for each individual IDE. For 11 microfluidic cartridges that were manufactured it was found that 35 IDEs had an RSD of within 17% for the measured electropolymerisation curves and 45 IDEs with an RSD of within 20%, this was higher than the best case within a single microfluidic cartridge. The electropolymerisation curves showed good similarities for IDEs two to five but a high level of inconsistencies for IDE one within the different microfluidic cartridges which is likely to arise from the IDE fabrication process. The inconsistencies for IDE one compared with the other IDEs was also subsequently indicated through the different impedimetric response of the bio-functionalised IDEs (Figure 6).

3.5 Clinical sample measurement

To demonstrate operation of the impedimetric reader with a microfluidic cartridge, containing the biofunctionalised IDEs, we tested the system with a middle range concentration of D-dimer in frozen plasma. The impedimetric reader follows a defined protocol for the clinical measurements. Firstly, the temperature of the cartridge is measured to check that this does not differ from predefined values. Baseline measurements are made in blank buffer (electrolyte) solution and measured values for the solution resistance (Rs), charge transfer resistance (Rct_{blank}) and double layer capacitance (Cdl) were determined from Nyquist plot measured with the developed reader. The clinical sample is then inserted into the sample reservoir of the microfluidic cartridge and pumped over the IDE array and left there for 15 minutes for ligand receptor binding. Buffer solution was then pumped via the septum on the microfluidic cartridge from a buffer reservoir to push back the clinical sample into the sample reservoir. This was used to clean the fluidic channel and minimise any interferents to the ligand receptor binding. The reader then makes further measurements for the Rs, Rct_{sample} and Cdl.

Given the previously determined inconsistencies for IDE one, this was not used for the measurement of D-dimer concentration within the clinical sample. As a means of improving the measurement accuracy the remaining four IDEs were used to make repeat measurements of D-dimer binding. Clinical samples containing D-dimer at a concentration of 437 ng/mL were measured over a total of 15 IDEs in different cartridges with a ratiometric percentage of sample reading against the blank with an average value of 124±15 with 95% confidence. This demonstrates that the developed microfluidic cartridge and impedimetric reader system is able to recognise D-dimer at a middle range concentration for IDEs within the microfluidic cartridge. Using the same receptor on each of the five IDE array elements within a single microfluidic cartridge will allow replication of measurements with internal standardisation and the potential for higher level of accuracy. Further work will be required to optimise fabrication of

the microfluidic cartridge to increase the reproducibility and decrease the failure rates as well as higher volume of testing for linearisation and quantification of this approach.

4.0 Conclusion

An array of biofunctionalised IDEs, within a microfluidic cartridge, and a portable impedimetric reader can be used for the measurement of D-dimer at a middle range concentration of a clinical plasma sample. The quality and reliability of the manufactured microfluidic cartridges can be monitored through a combination of optical microscopy, chronopotentiometry polymerisation curves and impedimetric analysis.

Biofunctionalisation with modified polypyrrole of the IDE array can be carried out in situ within a polymer microfluidic cartridge using chronopotentiometry with a 5μA current for a 50 second period and a two-electrode system with good reproducibility with RSD around 20%. This allows the immobilisation of His tag D-dimer antibody through NTA/ cooper complex attached to polypyrrole layer. The microfluidic cartridge was used to measure D-dimer in clinical sample at 437ng/mL using an impedimetric reader without amplification step and with results obtained in 15 minutes.

Future work will focus on improving the fabrication approach to increase reproducibility and decrease failure rates of the microfluidic cartridges for low cost label-free impedimetric POC diagnostics. Tailoring of the receptor on the IDE array would allow this approach to be applicable to a wide variety of diagnostic applications using impedimetric detection and without amplification.

Acknowledgements

This work was supported by European Commission through DVT-IMP project (project number 34256) and AL wishes to acknowledge the support of EPSRC through EP/K504609/1.

Credit Author Statement

The bulk of the experimental work was carried out by A. Lakey, S. Chebil, M. Kuphal, S. M. Scott, A. Ohlander and S. Hunor with supervision by Z. Ali, H.K-Youssoufi and J. Samitier Marti. The drafting of the manuscript was largely carried out by Z. Ali, H.K-Youssoufi, S. Hunor, M. Kuphal and S.M. Scott.

References

Anh, T.M., Dzyadevych, S. V., Van, M.C., Renault, N.J., Duc, C.N., Chovelon, J.-M., 2004. Conductometric tyrosinase biosensor for the detection of diuron, atrazine and its main metabolites. Talanta 63, 365–370. https://doi.org/10.1016/J.TALANTA.2003.11.008

Beckman, M.G., Hooper, W.C., Critchley, S.E., Ortel, T.L., 2010. Venous

Thromboembolism: A Public Health Concern. Am. J. Prev. Med. 38, S495–S501. https://doi.org/10.1016/J.AMEPRE.2009.12.017

Bourigua, S., Hnaien, M., Bessueille, F., Lagarde, F., Dzyadevych, S., Maaref, A., Bausells, J., Errachid, A., Renault, N.J., 2010. Impedimetric immunosensor based on SWCNT-COOH modified gold microelectrodes for label-free detection of deep venous thrombosis biomarker. Biosens. Bioelectron. 26, 1278–1282. https://doi.org/10.1016/j.bios.2010.07.004

Božič, M., Blinc, A., Stegnar, M., 2002. D-dimer, other markers of haemostasis activation and soluble adhesion molecules in patients with different clinical probabilities of deep vein thrombosis. Thromb. Res. 108, 107–114. https://doi.org/10.1016/S0049-3848(03)00007-0

Bucek, R.A., Quehenberger, P., Feliks, I., Handler, S., Reiter, M., Minar, E., 2001. Results of a New Rapid D-Dimer Assay (Cardiac D-Dimer) in the Diagnosis of Deep Vein Thrombosis. Thromb. Res. 103, 17–23. https://doi.org/10.1016/S0049-3848(00)00367-4

Chan, W.-S., Ginsberg, J.S., 2002. Diagnosis of deep vein thrombosis and pulmonary embolism in pregnancy. Thromb. Res. 107, 85–91. https://doi.org/10.1016/S0049-3848(02)00105-6

Chebil, S., Hafaiedh, I., Sauriat-Dorizon, H., Jaffrezic-Renault, N., Errachid, A., Ali, Z., Korri-Youssoufi, H., 2010. Electrochemical detection of d-dimer as deep vein thrombosis marker using single-chain d-dimer antibody immobilized on functionalized polypyrrole. Biosens. Bioelectron. 26. https://doi.org/10.1016/j.bios.2010.06.048

Chebil, S., Macauley, N., Hianik, T., Korri-Youssoufi, H., 2013. Multiwalled Carbon Nanotubes Modified by NTA-Copper Complex for Label-Free Electrochemical Immunosensor Detection. Electroanalysis 25, 636–643. https://doi.org/10.1002/elan.201200298

Cushman, M., Tsai, A.W., White, R.H., Heckbert, S.R., Rosamond, W.D., Enright, P., Folsom, A.R., 2004. Deep vein thrombosis and pulmonary embolism in two cohorts: the longitudinal investigation of thromboembolism etiology. Am. J. Med. 117, 19–25. https://doi.org/10.1016/J.AMJMED.2004.01.018

Ferguson, B.S., Buchsbaum, S.F., Swensen, J.S., Hsieh, K., Lou, X., Soh, H.T., 2009. Integrated Microfluidic Electrochemical DNA Sensor. Anal. Chem. 81, 6503–6508. https://doi.org/10.1021/ac900923e

Ghanima, W., Sandset, P.M., 2007. Validation of a new D-dimer microparticle enzyme immunoassay (AxSYM D-Dimer) in patients with suspected pulmonary embolism (PE). Thromb. Res. 120, 471–476. https://doi.org/10.1016/J.THROMRES.2006.11.005

Hafaid, I., Chebil, S., Korri-Youssoufi, H., Bessueille, F., Errachid, A., Sassi, Z., Ali, Z., Abdelghani, A., Jaffrezic-Renault, N., 2010. Effect of electrical conditions on an impedimetric immunosensor based on a modified conducting polypyrrole. Sensors Actuators, B Chem. 144. https://doi.org/10.1016/j.snb.2009.08.058

Ibupoto, Z.H., Jamal, N., Khun, K., Liu, X., Willander, M., 2013. A potentiometric

immunosensor based on silver nanoparticles decorated ZnO nanotubes, for the selective detection of d-dimer. Sensors Actuators B Chem. 182, 104–111. https://doi.org/10.1016/j.snb.2013.02.084

Ibupoto, Z.H., Mitrou, N., Nikoleli, G.-P., Nikolelis, D.P., Willander, M., Psaroudakis, N., 2014. The Development of Highly Sensitive and Selective Immunosensor Based on Antibody Immobilized ZnO Nanorods for the Detection of D-Dimer. Electroanalysis 26, 292–298. https://doi.org/10.1002/elan.201300580

Jaffrezic-Renault, N., Dzyadevych, S., 2008. Conductometric Microbiosensors for Environmental Monitoring. Sensors 8, 2569–2588. https://doi.org/10.3390/s8042569

Khadro, B., Santha, H., Nagy, P., Harsanyi, G., Jaffrezic-Renault, N., 2008. Comparison of the Performances of Conductometric Microsensors for Different Technologies and Designs of Interdigitated Electrodes. Sens. Lett. 6, 413–416. https://doi.org/10.1166/sl.2008.060

Korri-Youssoufi, H., Yassar, A., 2001. Electrochemical Probing of DNA Based on Oligonucleotide-Functionalized Polypyrrole. Biomacromolecules 2, 58–64. https://doi.org/10.1021/bm0000440

Kuphal, M., Mills, C.A., Korri-Youssoufi, H., Samitier, J., 2012. Polymer-based technology platform for robust electrochemical sensing using gold microelectrodes. Sensors Actuators, B Chem. 161, 279–284. https://doi.org/10.1016/j.snb.2011.10.032

Lopez, J.A., 2004. Deep Venous Thrombosis. Hematology 2004, 439–456. https://doi.org/10.1182/asheducation-2004.1.439

Marrakchi, M., Dzyadevych, S.V., Namour, P., Martelet, C., Jaffrezic-Renault, N., 2005. A novel proteinase K biosensor based on interdigitated conductometric electrodes for proteins determination in rivers and sewers water. Sensors Actuators B Chem. 111–112, 390–395. https://doi.org/10.1016/J.SNB.2005.03.099

Nikoleli, G.-P., Nikolelis, D.P., Tzamtzis, N., Psaroudakis, N., 2014. A Selective Immunosensor for D-dimer Based on Antibody Immobilized on a Graphene Electrode with Incorporated Lipid Films. Electroanalysis 26, 1522–1527. https://doi.org/10.1002/elan.201400161

Prodromidis, M.I., 2010. Impedimetric immunosensors—A review. Electrochim. Acta 55, 4227–4233. https://doi.org/10.1016/j.electacta.2009.01.081

Rackus, D.G., Shamsi, M.H., Wheeler, A.R., 2015. Electrochemistry, biosensors and microfluidics: a convergence of fields. Chem. Soc. Rev. 44, 5320–5340. https://doi.org/10.1039/C4CS00369A

Rodrigues, V.C., Moraes, M.L., Soares, J.C., Soares, A.C., Sanfelice, R., Deffune, E., Oliveira, O.N., 2018. Immunosensors Made with Layer-by-Layer Films on Chitosan/Gold Nanoparticle Matrices to Detect D-Dimer as Biomarker for Venous Thromboembolism. Bull. Chem. Soc. Jpn. 91, 891–896. https://doi.org/10.1246/bcsj.20180019

Rossier, J.S., Girault, H.H., 2001. Enzyme linked immunosorbent assay on a microchip

with electrochemical detection. Lab Chip 1, 153. https://doi.org/10.1039/b104772h

Santos, A., 2014. Fundamentals and Applications of Impedimetric and Redox Capacitive Biosensors. J. Anal. Bioanal. Tech. S7. https://doi.org/10.4172/2155-9872.S7-016

Srivastava, S.D., Eagleton, M.J., Greenfield, L.J., 2004. Diagnosis of pulmonary embolism with various imaging modalities. Semin. Vasc. Surg. 17, 173–180. https://doi.org/10.1053/J.SEMVASCSURG.2004.03.001

Tertiş, M., Ciui, B., Suciu, M., Săndulescu, R., Cristea, C., 2017. Label-free electrochemical aptasensor based on gold and polypyrrole nanoparticles for interleukin 6 detection. Electrochim. Acta 258, 1208–1218. https://doi.org/10.1016/j.electacta.2017.11.176

Triroj, N., Jaroenapibal, P., Shi, H., Yeh, J.I., Beresford, R., 2011. Microfluidic chip-based nanoelectrode array as miniaturized biochemical sensing platform for prostate-specific antigen detection. Biosens. Bioelectron. 26, 2927–2933. https://doi.org/10.1016/j.bios.2010.11.039

Zribi, B., Roy, E., Pallandre, A., Chebil, S., Koubaa, M., Mejri, N., Magdinier Gomez, H., Sola, C., Korri-Youssoufi, H., Haghiri-Gosnet, A.-M., 2016. A microfluidic electrochemical biosensor based on multiwall carbon nanotube/ferrocene for genomic DNA detection of Mycobacterium tuberculosis in clinical isolates. Biomicrofluidics 10, 014115. https://doi.org/10.1063/1.4940887

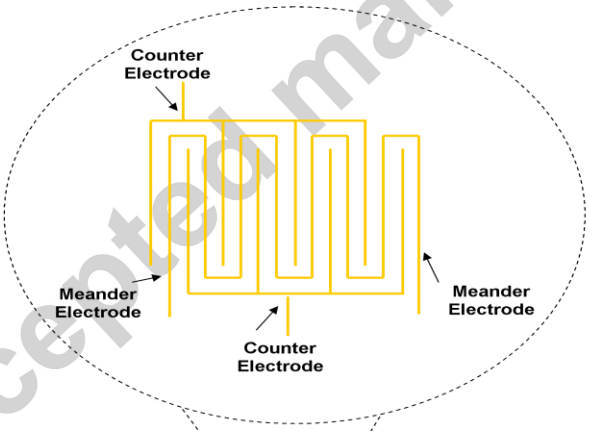

A

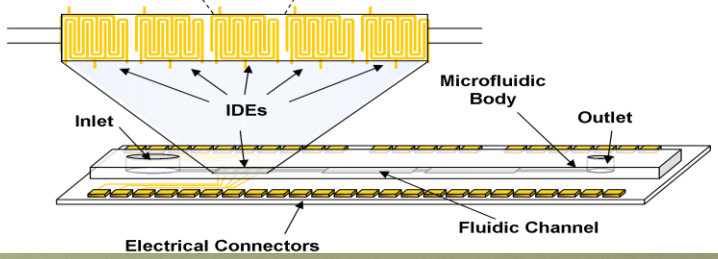

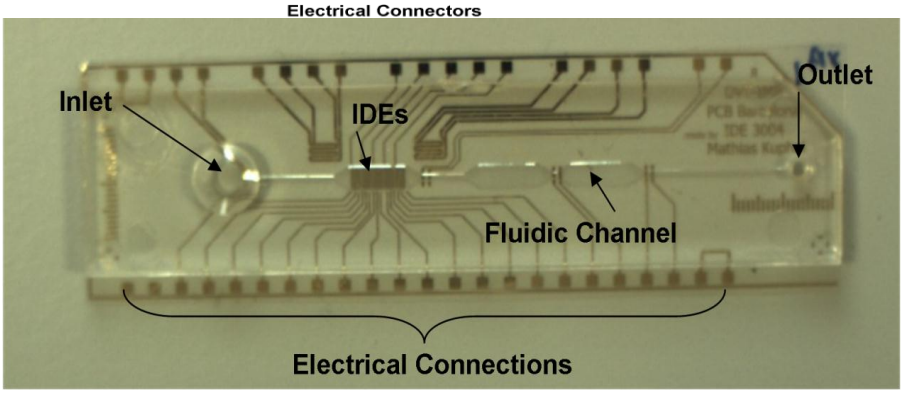

B

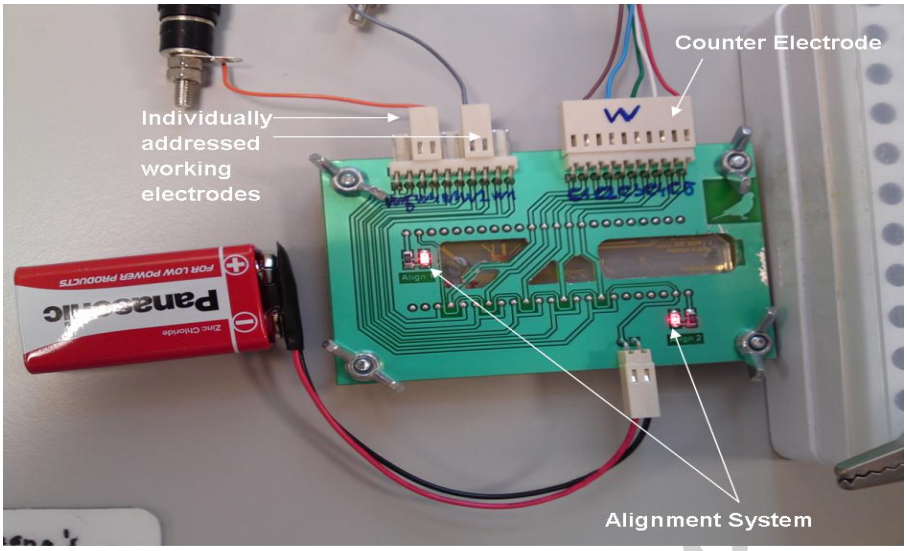

C

Figure 1 Photograph of the DVT/PE reader & alignment system (A) schematic representation of the IDE impedimetric array (B) microfluidic cartridge and (C) the microfluidic cartridge in connector frame.

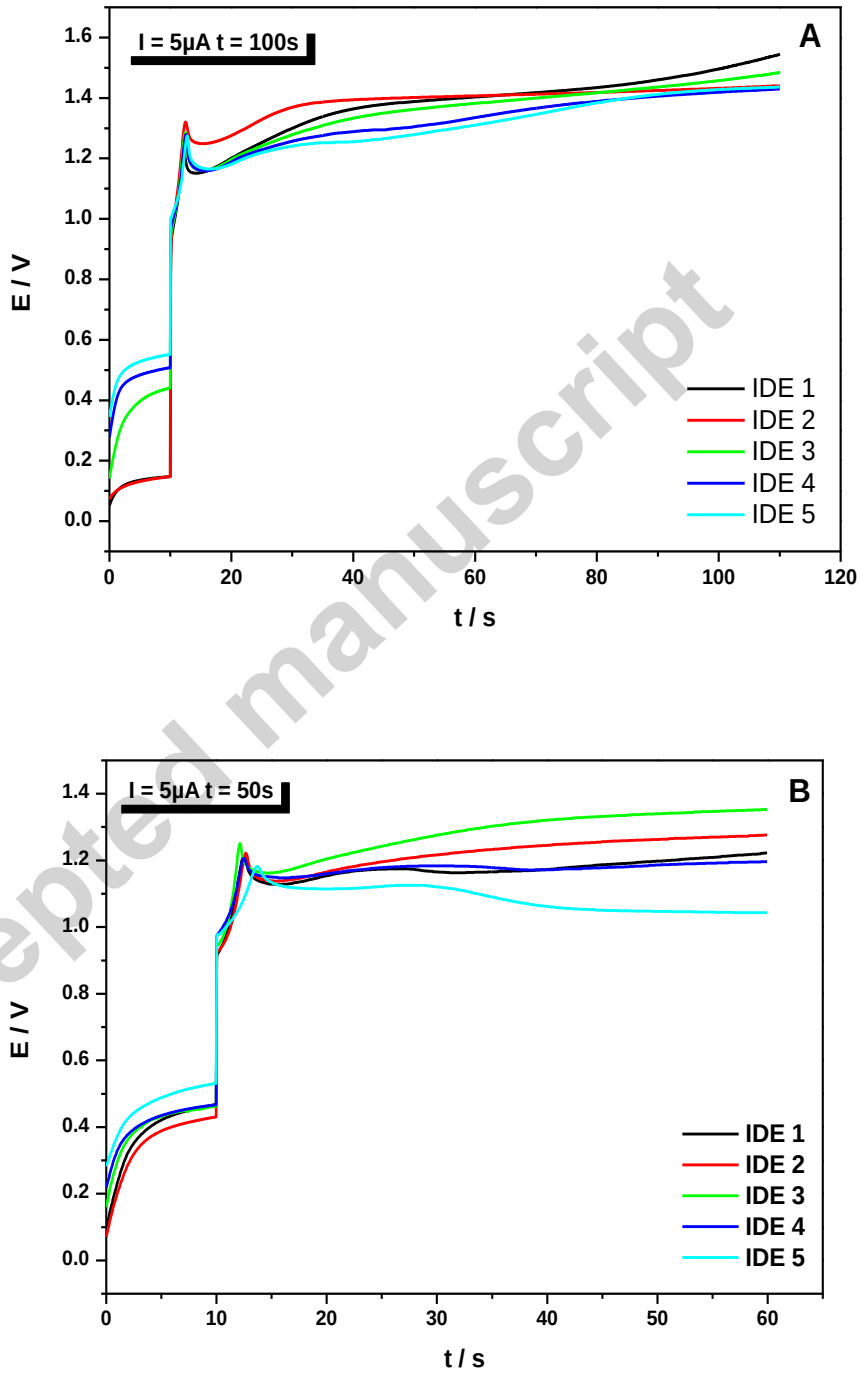

Figure 2 Chronopotentiometry ploymerization curves (5µA) for (A) 100 seconds (B) 50 seconds

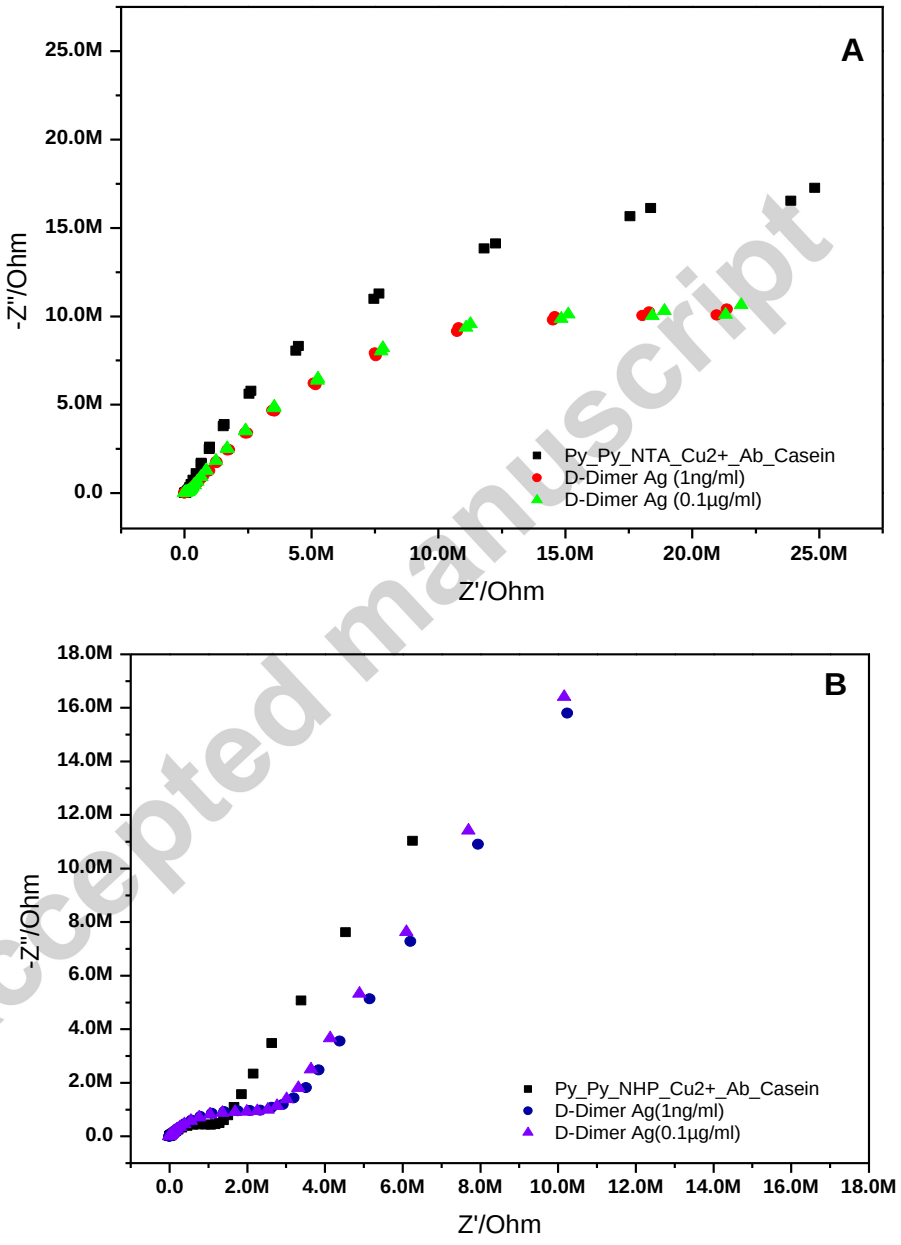

Figure 3 Nyquist plots showing the functionalised bio-layer and antibody-antigen interactions after polymerisation (A) 100 seconds (B) 50 seconds.

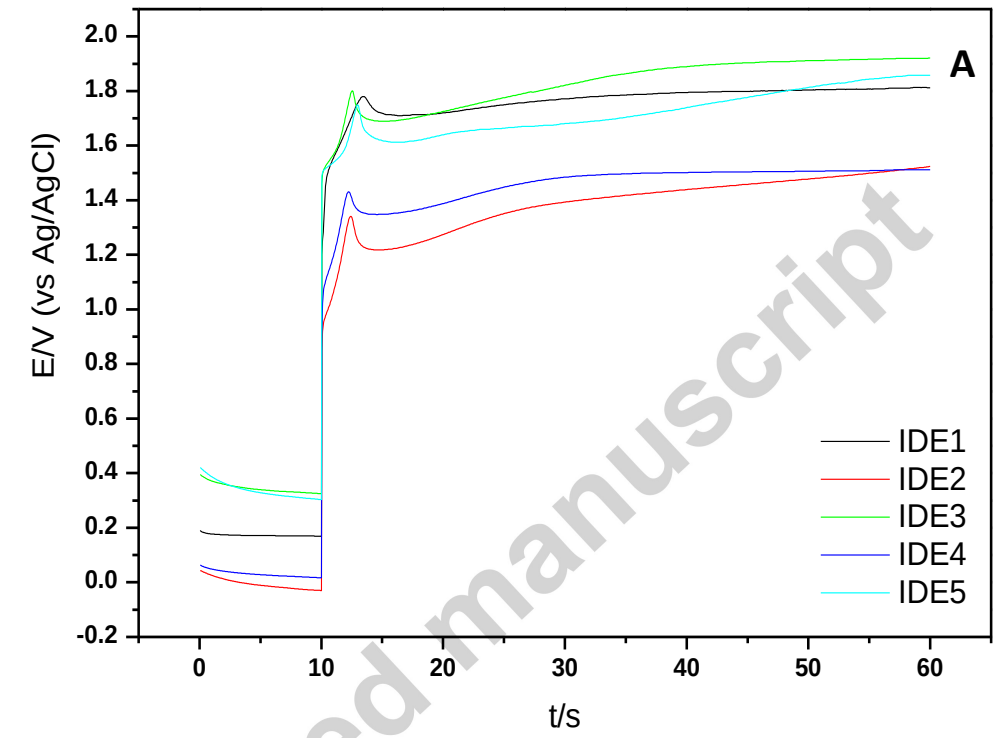

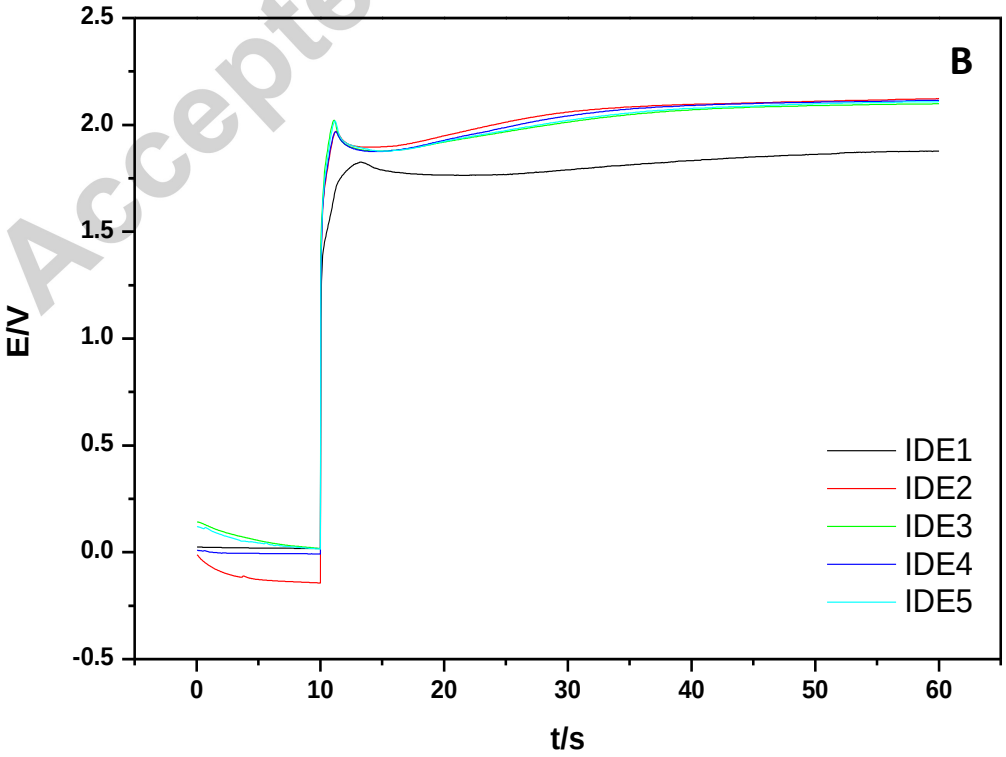

Figure 4 Electropolymerisation curves within microfluidic cartridge using (A) three electrode and (B) two electrode system.

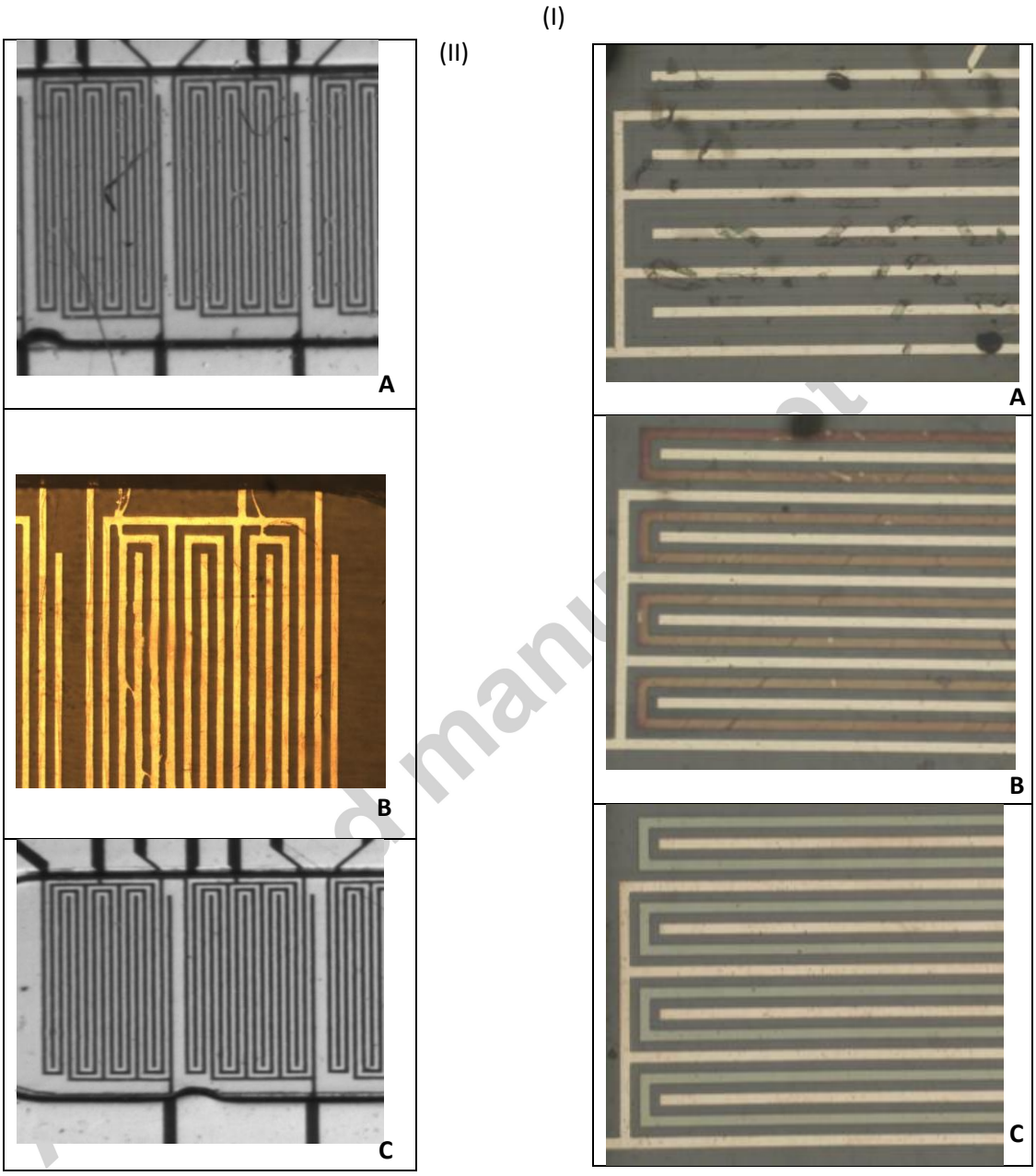

Figure 5 Microscope optical images of (I) bare IDEs showing (A) contamination (B) residual connections between the working and counter electrodes as result of incomplete etching (C) good quality (II) IDEs where meander has been bio-functionalised (A) meander delamination after deposition (B) inhomogeneous coating (C) biofunctionalised meander appears as a green coating.

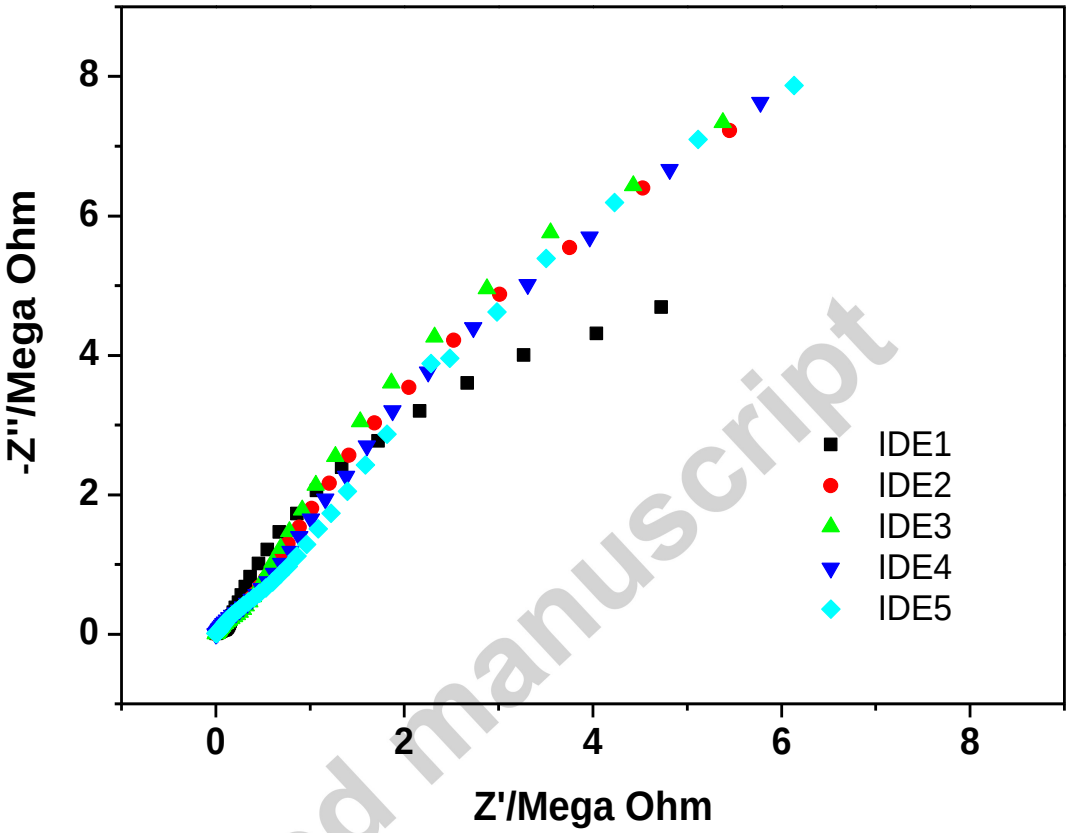

Figure 6 Nyquist plot showing the inconsistent biofunctionalisation of IDE one against the other IDEs within a typical microfluidic cartridge

Highlights

- Biofunctionalisation of IDE array in microfluidic device with electropolymerisation
- Portable impedimetric reader for detection of D-dimer biomarker
- Quality of biofunctionalisation monitored using optical microscopy
- Properties of biofunctionalised layers using chronopotentiometry and impedance
- Measurement of clinical plasma sample of four biofunctionalised IDEs